

Polarizer-free and fast response microlens arrays using polymer-stabilized blue phase liquid crystals

Yi-Hsin Lin, Hung-Shan Chen, Hung-Chun Lin, Yu-Shih Tsou, Hsu-Kuan Hsu, and Wang-Yang Li

Citation: *Applied Physics Letters* **96**, 113505 (2010); doi: 10.1063/1.3360860

View online: <http://dx.doi.org/10.1063/1.3360860>

View Table of Contents: <http://scitation.aip.org/content/aip/journal/apl/96/11?ver=pdfcov>

Published by the [AIP Publishing](#)

Articles you may be interested in

[A low voltage and submillisecond-response polymer-stabilized blue phase liquid crystal](#)

Appl. Phys. Lett. **102**, 141116 (2013); 10.1063/1.4802090

[Improved Kerr constant and response time of polymer-stabilized blue phase liquid crystal with a reactive diluent](#)

Appl. Phys. Lett. **102**, 071104 (2013); 10.1063/1.4793416

[Extended Kerr effect of polymer-stabilized blue-phase liquid crystals](#)

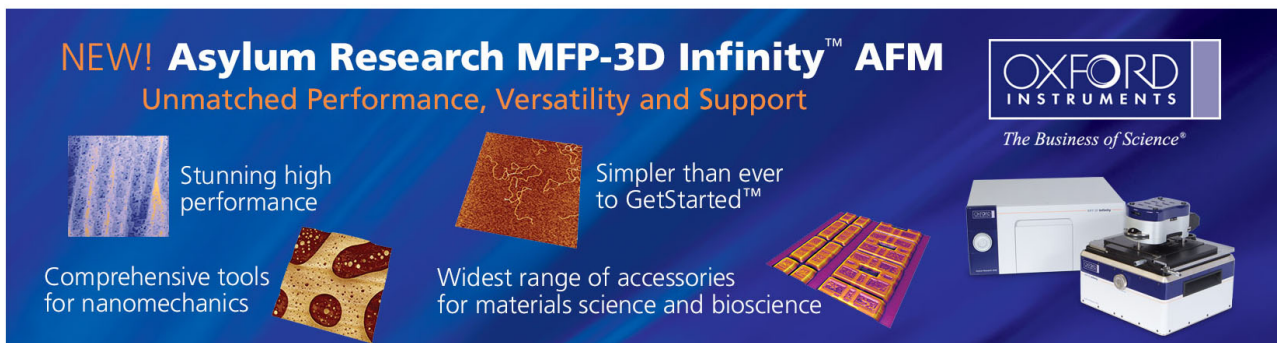
Appl. Phys. Lett. **96**, 071105 (2010); 10.1063/1.3318288

[A liquid crystalline polymer microlens array with tunable focal intensity by the polarization control of a liquid crystal layer](#)

Appl. Phys. Lett. **91**, 221113 (2007); 10.1063/1.2813638

[Polarization-independent and fast-response phase modulation using a normal-mode polymer-stabilized cholesteric texture](#)

J. Appl. Phys. **98**, 043112 (2005); 10.1063/1.2037191

The advertisement features a dark blue background with a grid of images showing various AFM scan results. The text is in white and orange. The Oxford Instruments logo is in the top right corner. The main headline is 'NEW! Asylum Research MFP-3D Infinity™ AFM' in white, with 'Unmatched Performance, Versatility and Support' in orange below it. The Oxford Instruments logo is in the top right corner, with the tagline 'The Business of Science®' below it. The advertisement highlights four key features: 'Stunning high performance' (with a scan image), 'Simpler than ever to GetStarted™' (with a scan image), 'Comprehensive tools for nanomechanics' (with a scan image), and 'Widest range of accessories for materials science and bioscience' (with a scan image). An image of the MFP-3D Infinity AFM system is shown in the bottom right corner.

Polarizer-free and fast response microlens arrays using polymer-stabilized blue phase liquid crystals

Yi-Hsin Lin,^{1,a)} Hung-Shan Chen,¹ Hung-Chun Lin,¹ Yu-Shih Tsou,¹ Hsu-Kuan Hsu,² and Wang-Yang Li²

¹Department of Photonics, National Chiao Tung University, Hsinchu 30010, Taiwan

²Chimei Optoelectronics Corp., Tainan 74147, Taiwan

(Received 14 January 2010; accepted 22 February 2010; published online 15 March 2010)

We demonstrate polarizer-free and fast response microlens arrays based on optical phase modulation of polymer-stabilized blue phase liquid crystal (PSBP-LC). Polarization-independent optical phase shift is because the propagation of an incident light is along the optic axis of PSBP-LC, and birefringence of PSBP-LC induced by Kerr effect results in electrically tunable optical phase shift. The measured optical phase shift of a PSBP-LC phase modulation is around π radian at 150 V_{rms} for the cell gap of 7 μ . The response time is about 3 ms. The focal length is around 13.1 cm at 100 V_{rms}. © 2010 American Institute of Physics. [doi:10.1063/1.3360860]

Liquid crystal (LC) phase-only modulations are electrically controllable without any mechanical moving parts, low cost, light weight, and low power consumption of LC phase modulations; as a result, LC phase modulations are widely used in adaptive optics, optical cross-connect switching, laser beam steering, and low-cost electro-optic sensors. The applications include self-adjusted eyeglasses, tunable-focus microlens arrays, electrically tunable gratings and prisms, and spatial light modulators.¹⁻⁴ However, the optical efficiency is limited due to utilizing a linear polarizer. Thus, to develop polarization-independent phase modulators is an urgent task. Two types of polarization independent phase modulators are developed.⁵ One is the residual phase type.⁶⁻⁸ All the LC directors have the same tilt angle except random orientations; as a result, all the polarizations of an incident light experience the same optical phase shift. The other type is double-layered structure.⁹⁻¹¹ The underlying principle is to stack two identical homogeneous LC layers together in orthogonal directions. An unpolarized light can be decomposed into two linear eigenpolarized lights. After propagating through the two stacked LC layers, both of eigenpolarized lights experience the same optical phase shift. The mechanisms of two types of polarization-independent phase modulations are based on the orientational change of LC directors. Recently, polymer-stabilized blue phase liquid crystals (PSBP-LCs) within wide temperature range attract many attentions, especially in the application of in-planed switching liquid crystal displays (IPS-LCDs) owing to fast response time, alignment-free, and wide viewing angle. Such IPS-LCDs require two polarizers because of optical anisotropy induced by the electric fields.¹²⁻¹⁵ In this paper, we demonstrate a polarizer-free and fast response microlens arrays based on the phase-only modulation of PSBP-LC. Polarization-independent optical phase shift is because the propagation of an incident light is along an optic axis of PSBP-LC, and the birefringence of PSBP-LC induced by Kerr effect results in electrically tunable optical phase shift. We discuss and measure the polarization-independent optical phase shift of the PSBP-LC. Then we measure the focusing properties of microlens arrays of PSBP-LCs.

Figure 1 illustrates the effective optical index-ellipsoids of the lens of PSBP-LC. The PSBP-LC is confined between two Indium Tin Oxide (ITO) glass substrates. At $V=0$, the effective optical index-ellipsoid of PSBP-LC is sphere which also means optical isotropic.^{12,15} When the applied voltage exceeds the critical voltage (V_c),¹⁶ the effective optical index-ellipsoid of PSBP-LC turns out ellipsoidal due to Kerr effect; moreover, the direction of the optic axis is parallel to z-direction. To obtain a lensing effect using PSBP-LC, we can apply an inhomogeneous electric field by patterned electrode with a circular aperture size (W) as shown in Fig. 1. In Fig. 1, the voltage is lower in the middle of the aperture and higher in the edge of the aperture. (i.e., $V_3 > V_2 > V_1$) The Kerr-effect-induced optic axes are parallel to z-direction and the effective optical index-ellipsoid turns out more elongated ellipsoid with higher voltage. PSBP-LC is optically isotropic for the unpolarized incident light propagating along the direction of the optic axis (or z direction). The refractive index of PSBP-LC is lower in the edge of the aperture; therefore, PSBP-LC forms a lenslike phase profile due to the spatial distribution of refractive indices. Such a lensing effect of PSBP-LC is polarization independent and electrically tunable. We can assume that, the refractive index of PSBP-LC is n_{ave} at $V_1=0$ for the unpolarized light. The refractive index of PSBP-LC is $n_{o,eff}(V)$ under applied voltage ($V > V_c$). The optical phase shift ($\Delta\delta$) between a high voltage (V) and $V=0$ can be expressed as,

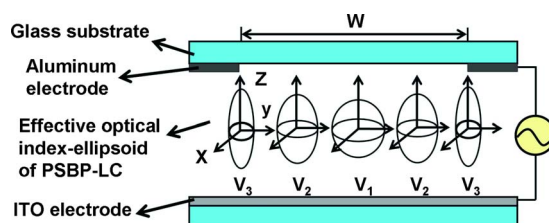


FIG. 1. (Color online) The effective optical index-ellipsoids of PSBP-LC under an inhomogeneous voltage distribution: $V_1=0$, $V_2(>V_c)$, and $V_3(>V_2)$. The incident light propagates along z-direction.

^{a)}Electronic mail: yilin@mail.nctu.edu.tw.

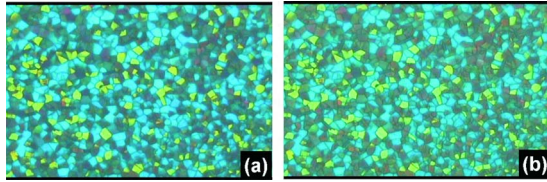


FIG. 2. (Color online) The morphologies of PSBPLC observing under a reflective polarizing optical microscopy at (a) 26 and (b) 38 °C.

$$\Delta\delta = \frac{2 \times \pi \times d}{\lambda} \times |n_{o,\text{eff}}(V) - n_{\text{ave}}(0)|, \quad (1)$$

where d is cell gap and λ is wavelength of the incident light. The incident light propagates along z -direction. The averaged refractive index at $0 V_{\text{rms}}$ for the small birefringence approximation can be expressed as,^{14,17}

$$n_{\text{ave}}(V=0) = \frac{2 \times n_o + n_e}{3}, \quad (2)$$

where n_o is ordinary refractive index of the host LC and n_e is extraordinary refractive index of the host LC. At $V \gg V_c$, $n_{o,\text{eff}}(V)$ is closed to n_o . Therefore, the optical phase shift between V_3 and V_1 from Eq. (1) turns out,

$$\Delta\delta = \frac{2 \times \pi \times d}{\lambda} \times \left| \frac{n_o - n_e}{3} \right|. \quad (3)$$

The phase shift of PSBP-LC depends on the cell gap, wavelength and birefringence ($n_e - n_o$) of host LC of PSBP-LC. The relation between the phase shift and the focal length (f) can be expressed as,²

$$f = \frac{\pi \times w^2}{4 \times \lambda \times |\Delta\delta|}. \quad (4)$$

To prepare the sample of PSBP-LC phase modulation, we mixed a positive nematic LC ($\Delta n = 0.142$) with two UV-curable monomers, EHA (2-Ethylhexyl, Fluka) and RM257 (Merck), a chiral molecules CB15 (Merck), and photoinitiator DMPAP (Aldrich) at 56.9:3.33: 3.42: 35.85: 0.5 wt % ratios. The mixture was prepared in Chimei Optoelectronics Corp. The mixture at isotropic state was filled into an empty LC cell consisting of two ITO glass substrates without any alignment layers and without circular pattern of ITO layers. The cell gap was 7 μm . We then cooled down the cell at the cooling rate of 0.1 °C/min, and the blue phase appeared at the temperature $T < 30$ °C. The cell was then exposed by UV light at 28.5 °C with intensity $\sim 1.5 \text{ mW/cm}^2$ for 30 min for photopolymerization. After photopolymerization, the PSBP-LC appeared blue phase when the temperature is between 20 and 41 °C.

In order to ensure the thermal stability and temperature range of PSBP-LC, we observed the morphologies of PSBP-LC with the temperature under a reflective polarizing microscopy without an applied voltage. Figure 2 shows the typical morphologies of PSBP-LC. In Fig. 2, the mosaic structures of PSBP-LCs at 26 and 38 °C are similar, but the color shifts slightly because the pitch and the birefringence of PSBP-LC are temperature-dependent. By the selective Bragg reflection and the Mozaic platelet structure, the domain size of PSBP-LC is around 20–50 μm . The PSBP-LC reflects light strongly in blue regime owing to the Bragg reflection. To avoid the blue regime for designing a

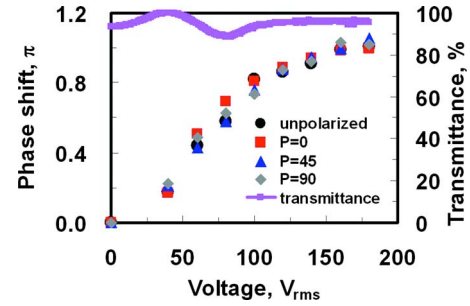


FIG. 3. (Color online) The transmittance (pink line) of PSBP-LC as a function of applied voltage under an unpolarized light. The optical phase shift of PSBP-LC as a function of an applied voltage under an unpolarized light (black dots), 0° linearly polarized light (red squares), 45° linearly polarized light (blue triangles), and 90° linearly polarized light (gray diamonds). $T = 26$ °C and $\lambda = 633 \text{ nm}$.

PSBP-LC phase modulation, we can either change the pitch of PSBP or shift the operating wavelength. In this paper, the operating wavelength of the following PSBP-LC phase modulation is set at 633 nm.

To evaluate the scattering properties of PSBP-LC, we measured voltage-dependent transmittance of PSBP-LC under an unpolarized He–Ne laser (JDSU Model 1122, $\lambda = 633 \text{ nm}$). The detector (New Focus Model 2031) was placed at 20 cm behind the PSBP-LC. To calibrate the substrate reflection losses, the transmittance of the BPLC at the isotropic state with the same cell gap is defined as unity. The measured results are shown in Fig. 3. In Fig. 3, the averaged transmittance is around 95% and the transmittance fluctuates slightly because of interference of multiple beams between two glass substrates. Hence, the PSBP-LC is almost scattering-free for the unpolarized red light.

To characterize the optical phase shift of the PSBP-LC, we used a Mach–Zehnder interferometer.⁹ The unpolarized He–Ne laser ($\lambda = 633 \text{ nm}$) was used as a light source. The PSBP-LC was driven by a square-wave voltage at frequency $f = 1 \text{ kHz}$. Figure 3 plots the measured optical phase shift as a function of an applied voltage under the unpolarized light (black dots). The optical phase shift increases when the voltage exceeds $V_c \sim 20 V_{\text{rms}}$. This is because the birefringence induced by Kerr effect increases with voltages; as a result, the difference of refractive indices between the high voltage and zero voltage increases. The shift of optical phase when we applied voltage is optical phase shift. The optical phase shift saturating at 150 V_{rms} is around $\sim \pi$ radian. In order to prove the optical phase modulation of PSBP-LC is indeed polarization independent, we placed a polarizer in front of the unpolarized laser and measured the optical phase shift by rotating the polarizer (P). The results are plotted in Fig. 3 (red squares, blue triangles, and gray diamonds). When we rotated the polarizer, we measured the same optical phase shifts. That means the phase shift is indeed independent of the polarization of the incident light. According to Eq. (3), $|\Delta\delta|$ can be calculated as $\sim 1.047\pi$ radian which is closed to the experimental result $\sim \pi$ radian. To increase the optical phase shift, high birefringence of host LC is preferred. Large cell gap can also enlarge the accumulation of the phase shift while maintaining the fast response time. However, larger cell gaps may result in the scattering and the non-uniform domains of PSBP-LC. To reduce the driving voltage, we can adopt the host BP-LC with high birefringence, large Kerr constant, large dielectric anisotropy

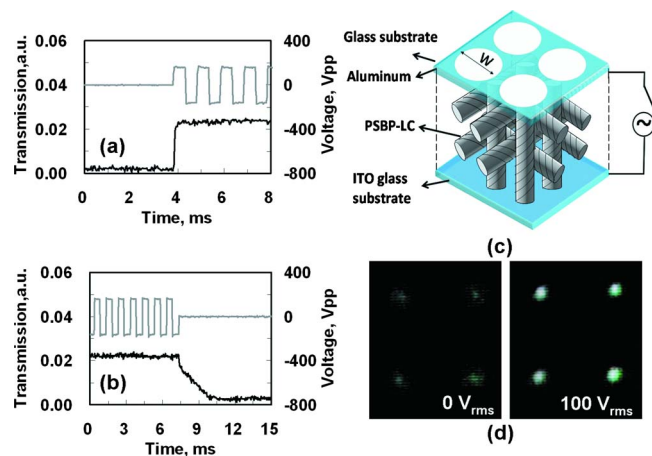


FIG. 4. (Color online) The transmission of PSBP-LC (black solid lines) and the corresponding squared ac voltage (gray lines) as a function of time. (a) The rising time is around 0.91 ms. (b) The decay time is around 2.3 ms. $T=26\text{ }^{\circ}\text{C}$ and $\lambda=633\text{ nm}$. (c) The structure of polarization independent microlens arrays using PSBP-LC. (d) Measured CCD images of 2D microlens arrays at 0 and 100 V_{rms} , $T=26\text{ }^{\circ}\text{C}$ and $\lambda=532\text{ nm}$.

($\Delta\epsilon$), and large ratio of bend elastic constant (K_{33}) to splay elastic constant (K_{11}).^{18–20} The response time is also important for phase modulators. The measured response times are shown in Figs. 4(a) and 4(b). The rise time is $\sim 0.91\text{ ms}$ and decay time is $\sim 2.3\text{ ms}$. Compared to the conventional pure-LC phase modulation whose response time ($\sim 200\text{ ms}$) (Ref. 9) proportional to d^2 , the faster response time of PSBP-LC is because of orientation of local LC directors within the unit lattice rather than the transition between two nematic orientations of LC directors with higher order parameters.^{12,13} Compared to the typical response time of PSBP-LC less than 1 ms, the slower response time of our PSBP-LC is because the pitch length of PSBP-LC is long.²¹

To demonstrate a two-dimensional (2D) microlens arrays using PSBP-LC as an electro-optics medium, we prepared the microlens arrays consisting of one ITO glass substrate, one glass substrate coating with an aluminum layer which was etched hole-patterns of $250\text{ }\mu\text{m}$ in diameter and PSBP-LC, as shown in Fig. 4(c). The cell gap was $20\text{ }\mu\text{m}$. To characterize the focusing properties, a collimated unpolarized light at $\lambda=532\text{ nm}$ was used to illuminate the PSBP-LC microlens arrays. The transmitted light was recorded by a charge-coupled device (CCD). The recorded images at $V=0$ and $V=100\text{ }V_{\text{rms}}$ are shown in Fig. 4(d). At $V=0$, no focus was observed. At $V=100\text{ }V_{\text{rms}}$, PSBP-LC microlens arrays showed clear focal spots. The tunable focal length was measured from infinity at $V=0$ to 13.1 cm at $100\text{ }V_{\text{rms}}$. When we placed a polarizer in front of the microlens arrays, the measured focal length did not change with the rotation of polarizer. In Fig. 3, $\Delta\delta$ is $\sim 0.2\pi$ radian at $5\text{ }V_{\text{rms}}/\mu\text{m}$ at $\lambda=633\text{ nm}$. As a result, $\Delta\delta$ is $\sim 0.238\pi$ radian at $\lambda=532\text{ nm}$. The calculated focal length is 12.34 cm which is closed to the measured focal length of 13.1 cm. The operating voltage is high and focal length is quite long owing to the small Kerr constant of PSBP-LC ($\sim 10^{-10}\text{ m/V}^2$). Due to

the Bragg reflection and the scattering, the transmittance is around 86% for $\lambda=532\text{ nm}$. To improve the transmittance, we can shift the pitch of PSBPLC or use the incident light with the wavelength of 633 nm.

In conclusion, we have demonstrated polarizer-free, fast response, and alignment-layer-free microlens arrays based on phase modulation of PSBP-LC. The optical phase shift of PSBP-LC is polarization independent and electrically tunable. The focal length is around 13.1 cm at $100\text{ }V_{\text{rms}}$ with the response time of $\sim 3\text{ ms}$. To enlarge the tunable focusing range, we can increase the optical phase shift by enlarging the essential birefringence of host BPLC. Unlike the nematic LC based phase modulation, the increase of cell gap of PSBP-LC can accumulate optical phase shift, but do not increase response time dramatically. We believe the polarization independent phase modulation of PSBP-LC opens a window for photonic microdevices.

The authors are indebted to Dr. Yung-Hsun Wu (Innolux Display Corp.), Mr. Tsung-Han Chiang, Mr. Chun-Hung Wu for discussions, Professor Hung-Chou Lin (MSE, NCTU), and Ms Hsiao-Ping Fang (MSE, NCTU) for the measurement of Differential Scanning Calorimetry. This research was supported by Chimei Optoelectronics Corp. and by the National Science Council (NSC) in Taiwan under the Contract No. 98-2112-M-009-017-MY3.

¹D. K. Yang and S. T. Wu, *Fundamentals of Liquid Crystal Devices* (Wiley, New York, 2006).

²H. Ren, Y. H. Fan, S. Gauza, and S. T. Wu, *Appl. Phys. Lett.* **84**, 4789 (2004).

³Y. H. Lin, H. Ren, K. H. Fang-Chiang, W. K. Choi, S. Gauza, X. Zhu, and S. T. Wu, *Jpn. J. Appl. Phys., Part 1* **44**, 243 (2005).

⁴H. Ren, Y. H. Fan, and S. T. Wu, *Appl. Phys. Lett.* **82**, 3168 (2003).

⁵Y. H. Lin, H. Ren, and S. T. Wu, *Liq. Cryst. Today* **17**, 2 (2009).

⁶H. Ren, Y. H. Lin, Y. H. Fan, and S. T. Wu, *Appl. Phys. Lett.* **86**, 141110 (2005).

⁷Y. H. Lin, H. Ren, Y. H. Fan, Y. H. Wu, and S. T. Wu, *J. Appl. Phys.* **98**, 043112 (2005).

⁸H. Ren, Y. H. Lin, C. H. Wen, and S. T. Wu, *Appl. Phys. Lett.* **87**, 191106 (2005).

⁹Y. H. Lin, H. Ren, Y. H. Wu, Y. Zhao, J. Y. Fang, Z. Ge, and S. T. Wu, *Opt. Express* **13**, 8746 (2005).

¹⁰H. Ren, Y. H. Lin, and S. T. Wu, *Appl. Phys. Lett.* **88**, 061123 (2006).

¹¹Y. Huang, C. H. Wen, and S. T. Wu, *Appl. Phys. Lett.* **89**, 021103 (2006).

¹²H. Kikuchi, M. Yokota, M. Hisakado, H. Yang, and T. Kajiyama, *Nature Mater.* **1**, 64 (2002).

¹³Y. Hisakado, H. Kikuchi, T. Nagamura, and T. Kajiyama, *Adv. Mater.* **17**, 96 (2005).

¹⁴H. S. Kitzerow, *Proc. SPIE* **7232**, 723205 (2009).

¹⁵Y. Haseba, H. Kikuchi, T. Nagamura, and T. Kajiyama, *Adv. Mater.* **17**, 2311 (2005).

¹⁶K. M. Chen, S. Gauza, H. Xianyu, and S. T. Wu, *J. Disp. Technol.* **6**, 49 (2010).

¹⁷J. Li, S. Gauza, and S. T. Wu, *J. Appl. Phys.* **96**, 19 (2004).

¹⁸S. W. Choi, S. I. Yamamoto, Y. Haseba, H. Higuchi, and H. Kikuchi, *Appl. Phys. Lett.* **92**, 043119 (2008).

¹⁹Z. Ge, S. Gauza, M. Jiao, H. Xianyu, and S. T. Wu, *Appl. Phys. Lett.* **94**, 101104 (2009).

²⁰L. Rao, Z. Ge, S. T. Wu, and S. H. Lee, *Appl. Phys. Lett.* **95**, 231101 (2009).

²¹P. R. Gerber, *Mol. Cryst. Liq. Cryst.* **116**, 197 (1985).